Surface Integrity-Informed CPFEM: A Novel Approach to the Prediction of Fatigue Crack Initiation in Ti-6Al-4V

M.F. Arcidiacono[1a], I. Violatos[1] and S. Rahimi[1]

[1]Advanced Forming Research Centre (AFRC), University of Strathclyde 85 Inchinnan Drive, Inchinnan, Renfrewshire, UK

[a]mauro.arcidiacono@strath.ac.uk

Introduction

Titanium and its alloys, renowned for their high strength-to-density ratio, corrosion resistance, biocompatibility, and resistance to fractures, are widely used in aerospace, astronautics, and biomedical engineering. In particular, most of the production of Titanium and its alloys is for the aerospace industry [1], where parts are manufactured via sequential thermomechanical processes, often followed by machining. The most commonly used alloy is the dual phase $\alpha + \beta$ Ti-6Al-4V, which has good producibility and an optimal balance of ductility, strength, and fatigue and fracture resistance [2]. Ti-6Al-4V is used to produce critical aerospace components, such as airframe parts, and compressor disks and blades of the jet engine [3] [4]. Notably, many aerospace components are affected by repeated loading, dwell and unloading cycles. Fatigue crack initiation and propagation, resulting from high cycle fatigue (HCF), is a common form of damage observed in Ti-6Al-4V compressor blades and disks. Surface integrity is a key factor in fatigue initiation and propagation since it exerts a significant effect on performance, life and reliability [5]. Therefore, this work aims to present a surface integrity-informed Crystal Plasticity Finite Element Method (CPFEM) model to estimate fatigue crack initiation in Ti-6Al-4V as a function of milling parameters. The proposed approach uses experimental microstructural and surface integrity data (i.e., roughness and residual stress) to perform the analyses.

Methodology

Two 30 mm thickness plates of aerospace grade Ti-6Al-4V were extracted from an as-forged and heat treated part, which was ready for its final machining operation. Three finishing milling passes with a machining depth of 0.3 mm were carried out with three different feeds per tooth using a DMG Mori CNC machine. The selected feed speeds at machine diameter to evaluate the effect of different cutting conditions were 663, 738, 811 mm/min, referenced as cut A, B and C, respectively. Cut B aligns with the feed recommended by the manufacturer of the cutting tools. The spindle speed was 461/min and the cutting tool was equipped with 4 inserts. A Kistler Dynamometer Type 9139AA and a Spike pro-micron were used to measure cutting forces and torques in the part and in the cutting tool, respectively.

After machining, the roughness (R_a and R_z) was measured considering a cutoff value of 2.5 mm using a HIROX optical microscope in selected sites across and along the milled paths. In-plane surface residual stresses were measured with X-ray diffraction (XRD) to acquire information of the post-milling stress state. To obtain near-surface residual stress data, Electron Speckle Pattern Interferometry (ESPI) coupled with hole-drilling was implemented in the centre of the cutting path.

To further characterise surface integrity, a set of samples were extracted from each cutting path and a Knoop microhardness test was performed to evaluate the change in hardness due to the deformation induced by milling. Light Optic Microscopy (LOM), Scanning Electron Microscopy (SEM) and Electron Backscattered Diffraction (EBSD) were used to analyse the microstructure and the deformed layer due to machining.

The experimental characterisation data were digitalised through an in-house computational framework and integrated with simulated data from milling; the processing steps are shown in Fig. 1. The mechanical response of the material was modelled using a crystal plasticity framework and the fatigue initiation was analysed by calculating physically-based fatigue initiation parameter (FIP) fields.

Results and Discussion

The dynamometer measured the highest cutting forces during the cut with the highest feed per tooth and, in that condition, the maximum measured force was that of the out of plane direction. On average, the lowest forces were registered in cut B. The minimum average of R_a was 10.28 μm in cut B, however the difference between the maximum and minimum values was only 2.84%. As can be observed in Fig. 2, the maximum R_a measured difference in the centre of the cut was in the radial direction in cut C, while the minimum difference in that direction was in cut A.

The in-plane normal residual stresses measured with XRD were compressive, while the shear stresses were negligible. Fig. 2 shows that the variance of the stresses is lower in the radial direction than in the cutting direction. The compressive stresses are lower at the centre of the cut path in the cutting direction, due to the velocity of the inserts being perpendicular to this orientation. The disparity between the normal stresses in the cutting direction at the edges of the path versus the centreline may arise from the interplay between the tool's rotational and linear motions. On one side of the cutting path, the tool's radial angular velocity is aligned with the tool's traverse movement (direction of milling), effectively increasing the local engagement velocity of the

cutter with the material. Conversely, on the opposite side, the velocity is lower since the radial angular and linear traverse velocities are exactly opposite. This difference might have led to asymmetric normal stresses as measured and shown in Fig. 2.
Micromechanical simulation results indicate that fatigue crack initiation is linked with the surface topology, residual stresses and strains resulting from previous machining operations. Furthermore, the proposed Finite Element Method (FEM) model suggested that local crystallographic effects and morphology also affect fatigue crack formation in Ti-6Al-4V.

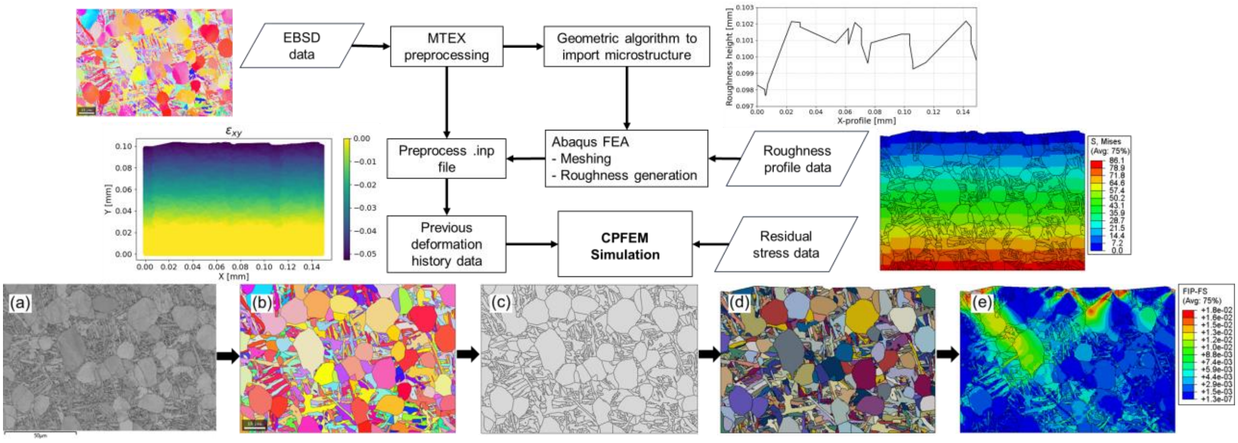

Figure 1. Processing steps from (a) to (d) to digitalise microstructural data and integrate them into the micromechanical CPFEM model.

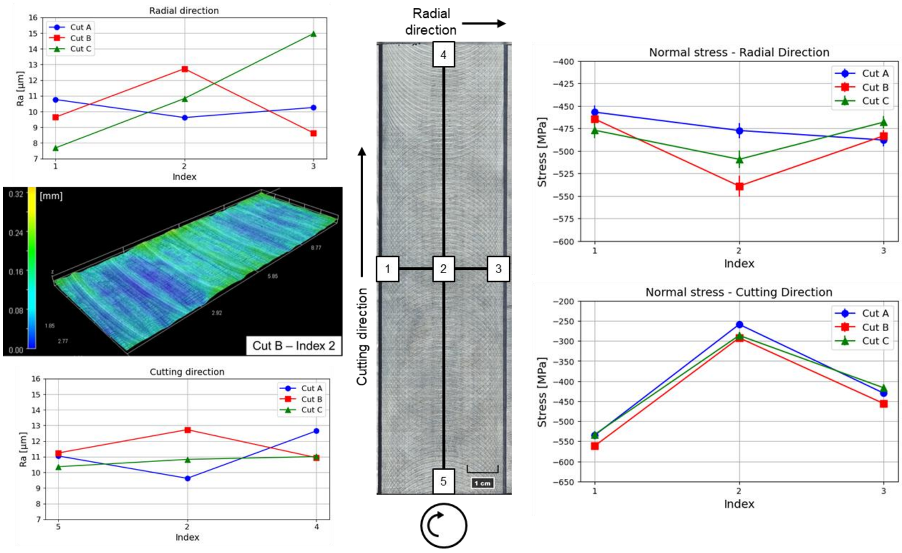

Figure 2. Average roughness and surface stresses in the radial and cutting directions for each cut.

Conclusion

The set of parameters selected to machine a part influence the surface integrity, i.e., the roughness, residual stresses and accumulated strain modifying the mechanical response of the component in service. Milling also causes deformed microstructures at a subsurface layer, therefore, affecting the mechanical response of the material to fatigue. Consequently, by analysing the key parameters influencing surface integrity post-machining, CPFEM models can not only increase predictive accuracy and understanding of fatigue crack initiation in Ti-6Al-4V, but also guide the optimisation of milling parameters to increase the final part's resistance to fatigue crack initiation.

References

[1] M. El Khalloufi, O. Drevelle, and G. Soucy: *Titanium: An overview of resources and production methods*, Minerals, Vol. 11 (2021), 1425.

[2] Gerd Lütjering and James C. Williams: *Titanium*, Springer Berlin, Heidelberg (2007).

[3] R. K. Gupta, V. A. Kumar, C. Mathew, and G. S. Rao: *Strain hardening of Titanium alloy Ti6Al4V sheets with prior heat treatment and cold working*, Mater. Sci. Eng. A., Vol. 662, p. 537-550 (2016)

[4] C. Veiga, J. P. Davim, and A. J. R. Loureiro: *Properties and applications of titanium alloys: a brief review*, Rev. Adv. Mater. Sci., Vol. 32 (2012), p. 14-34.

[5] M. Brown, D. Wright, R. M'Saoubi, J. McGourlay, M. Wallis, A. Mantle, P. Crawforth and H.Ghadbeigi: *Destructive and non-destructive testing methods for characterization and detection of machining-induced white layer*: *A review paper*, CIRP-JMST, Vol. 23 (2018), p. 39–53.